SUPPLEMENTAL DATA

Sup. Fig. 1. Biophysical properties of WT and charge-neutralized mutant Kv2.1 channels. (A) Whole cell current recordings of WT Kv2.1 (○), Kv2.1 (C73A) (♦), Kv2.1(D74A) (▲), Kv2.1(D75A) (●) and Kv2.1(D74-75A) (■). The voltage protocol is given on top and the scale bar in each recording represents 0.2 s and 0.2 nA. (B) Voltage dependence of activation. The activation curve was obtained from the normalized tail current amplitudes in panel A as a function of the prepulse potential and fitted with a Boltzmann function (solid line). (C) Voltage dependence of inactivation. The inactivation curve was derived from the normalized peak current amplitude at 60 mV after a 5-sec prepulse plotted as a function of the prepulse potential. (D) Time constants of activation and deactivation, obtained from a single or double exponential fit of the raw current recordings. (E) Current density of WT and mutant channels determined at the end of a 500-ms step to +30 mV. Expression levels were defined after transfection of 50 ng channel DNA and overnight incubation at 37°C. The numbers above every bar indicate the number of cells analyzed. Note that the biophysical properties of the different charge-neutralized Kv2.1 mutants were similar to WT Kv2.1. However, the current densities of Kv2.1(D74A) and especially of the double mutant Kv2.1(D74-75A) were reduced compared to WT Kv2.1 which was statistically significant (*, $p < 0.05$) for Kv2.1(D74-75A). This reduction was abolished by transfection of a 10-fold higher amount of Kv2.1(D74-75A) cDNA (i.e. 0.5 µg) which resulted in a current density of 152 ± 61 pA/pF (n =4); not significant vs. WT.

Sup. Fig. 2. Illustration of a YFP-CFP dimer and the YFP emission spectrum upon excitation with 458nm laser. (A) Illustration of one of the many possible orientations of both the YFP and CFP molecules in a dimeric construct, created by linking the separate 3D crystal structures. Such YFP-CFP dimer construct was used as a positive control for the FRET measurements and resulted in a FRET efficiency of 38.5 ± 1.5 % (n = 18). Based on the R_o of 49.2 Å for an YFP-CFP pair, this efficiency corresponds to an YFP-CFP fluorophore separation of 52.9 ± 0.8 Å. Given the constraints of the molecular size and the location of the active chromophores in the center of the molecules (highlighted in yellow and cyan with their solvent accessible surface added), the experimentally obtained distance agreed quite well with the expected separation of the active chromophores in an YFP-CFP dimer. (B) Average normalized YFP emission fluorescence spectra of 5 separate cells expressing YFP that were excited with 458nm laser light. Analysis of this YFP emission spectra showed that the fluorescence emission in the bandwidth 464-490nm was limited to less than 0.1%. This indicated that there was virtually no bleed through of YFP emission fluorescence in the CFP bandwidth that was used for measuring FRET efficiencies.

Sup. Table 1. Biophysical properties of WT and charge-neutralized mutant Kv2.1 channels. Values are given as mean ± SEM. N represents the number of cells analyzed. The midpoints of activation and inactivation ($V_{1/2}$) and both slope factors (k) were obtained from a single Boltzmann fit (see experimental procedures). Time constants (Tau) of activation and deactivation were obtained from fitting current activation and deactivation with a single or double exponential function, respectively.

Supplemental Figure 1

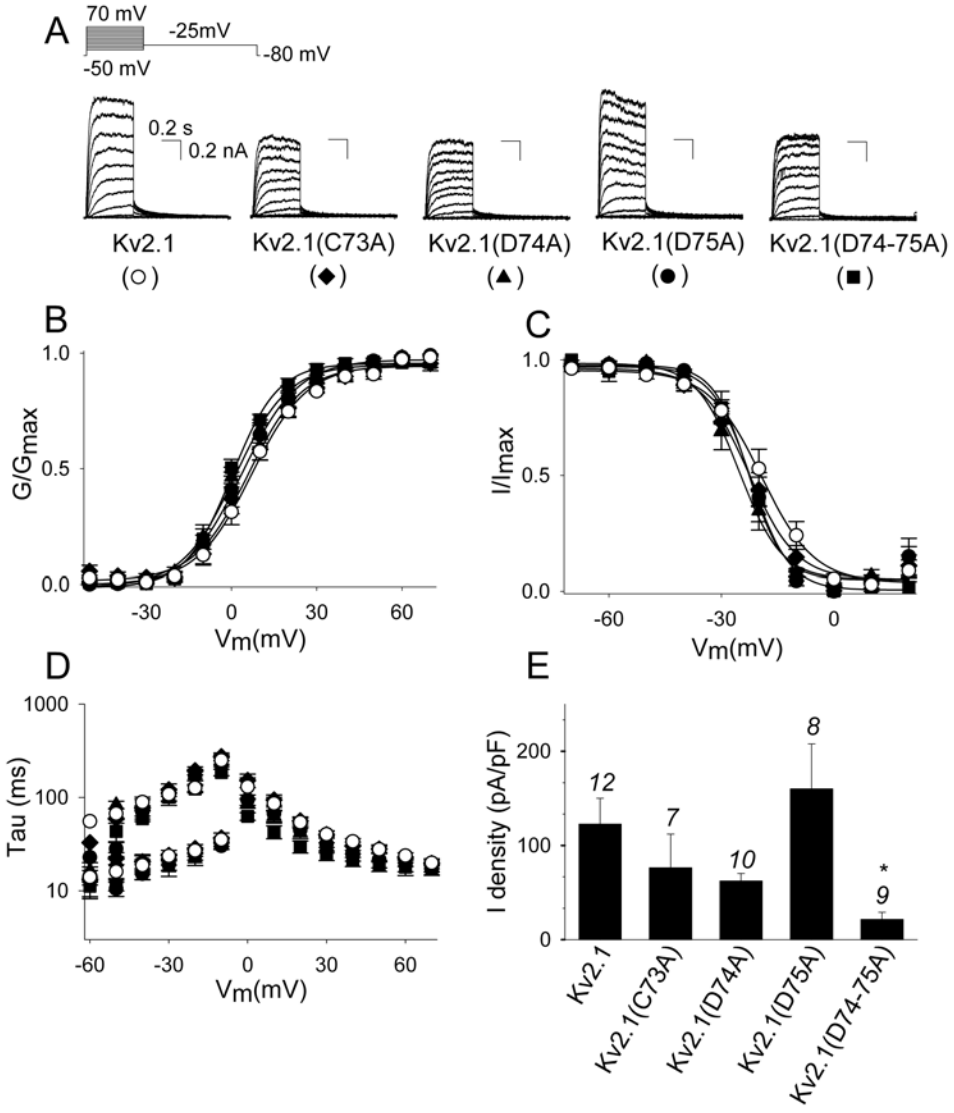

Supplemental Figure 2

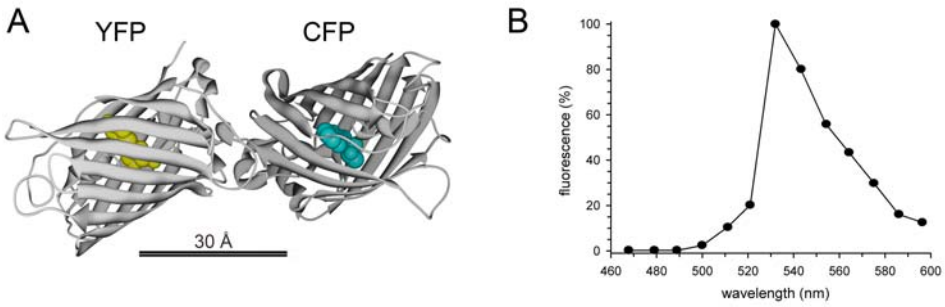

Supplemental Table 1

	Kv2.1	Kv2.1 (C73A)	Kv2.1 (D74A)	Kv2.1 (D75A)	Kv2.1 (D74-75A)
Activation					
$V_{1/2}$	6.1 ± 2.2	5.7 ± 1.3	1.0 ± 1.7	2.4 ± 2.6	-0.1 ± 1.4
slope	9.0 ± 0.4	9.2 ± 0.5	9.2 ± 0.8	8.4 ± 0.4	8.3 ± 0.7
Tau (60 mV)	23.7 ± 1.8	22.8 ± 2.7	19.9 ± 1.7	19.4 ± 3.4	17.9 ± 3.3
n	7	7	6	8	4
Inactivation					
$V_{1/2}$	-18.2 ± 2.3	-21.7 ± 2.1	-24.3 ± 2.4	-22.0 ± 0.8	-22.3 ± 2.0
slope	6.4 ± 0.5	6.4 ± 0.6	5.7 ± 0.4	5.1 ± 0.1	5.0 ± 0.2
n	7	6	4	4	3
Deactivation					
Tau 1 (-20 mV)	26.9 ± 1.8	28.4 ± 2.9	22.0 ± 3.4	25.1 ± 1.8	23.1 ± 0.8
Tau 2 (-20 mV)	126.8 ± 10.8	193.2 ± 18.7	174.6 ± 24.3	170.6 ± 18.2	123.1 ± 10.8
n	6	4	4	5	4